Bacillus subtilis chromosome organization oscillates between two distinct patterns

Xindan Wang, Paula Montero Llopis, and David Z. Rudner[1]

Department of Microbiology and Immunobiology, Harvard Medical School, Boston, MA 02115

Bacterial chromosomes have been found to possess one of two distinct patterns of spatial organization. In the first, called "ori-ter" and exemplified by *Caulobacter crescentus*, the chromosome arms lie side-by-side, with the replication origin and terminus at opposite cell poles. In the second, observed in slow-growing *Escherichia coli* ("left-*ori*-right"), the two chromosome arms reside in separate cell halves, on either side of a centrally located origin. These two patterns, rotated 90° relative to each other, appear to result from different segregation mechanisms. Here, we show that the *Bacillus subtilis* chromosome alternates between them. For most of the cell cycle, newly replicated origins are maintained at opposite poles with chromosome arms adjacent to each other, in an *ori-ter* configuration. Shortly after replication initiation, the duplicated origins move as a unit to midcell and the two unreplicated arms resolve into opposite cell halves, generating a left-*ori*-right pattern. The origins are then actively segregated toward opposite poles, resetting the cycle. Our data suggest that the condensin complex and the *parABS* partitioning system are the principal driving forces underlying this oscillatory cycle. We propose that the distinct organization patterns observed for bacterial chromosomes reflect a common organization–segregation mechanism, and that simple modifications to it underlie the unique patterns observed in different species.

DNA replication | ParA | chromosome segregation | SMC condensin

Central to reproduction is the faithful segregation of replicated chromosomes to daughter cells. In eukaryotes, DNA replication, chromosome condensation, and sister chromatid segregation are separated into distinct steps in the cell cycle that are safeguarded by checkpoint pathways. In bacteria, these processes occur concurrently, posing unique challenges to genome integrity and inheritance (1, 2). In the absence of temporal control, bacteria take advantage of spatial organization to promote faithful and efficient chromosome segregation. The organization of the chromosome dictates where the chromosome is replicated, and the factors that organize and compact the newly replicated DNA play a central role in its segregation (1, 2).

Studies in different bacteria have revealed strikingly distinct patterns of chromosome organization that appear to arise from different segregation mechanisms. In *Caulobacter crescentus* and *Vibrio cholerae* chromosome I, the origin and terminus are located at opposite cell poles, with the two replication arms between them, in a pattern referred to as "*ori-ter*" (3–5). After replication initiation, one of the sister origins is held in place and the other is actively translocated to the opposite cell pole, regenerating the *ori-ter* organization in both daughter cells (5–11). By contrast, in slow-growing *Escherichia coli*, the origin is located in the middle of the nucleoid and the two replication arms reside in opposite cell halves, in a "left-*ori*-right" pattern (12, 13). Replication initiates at midcell, and the duplicated origins segregate to the quarter positions followed by the left and right arms on either side, regenerating the left-*ori*-right pattern in the two daughter cells.

Although chromosome organization was first analyzed in the Gram-positive bacterium *Bacillus subtilis*, our understanding of the replication–segregation cycle in this bacterium has remained elusive. In pioneering studies, it was shown that during spore formation, the replicated origins reside at opposite cell poles and

the termini at midcell in an *ori-ter ter-ori* organization (14–18). A similar *ori-ter* pattern was observed during vegetative growth (15, 19). However, in separate studies, DNA replication was found to initiate at a midcell-localized origin (20, 21). How these disparate patterns fit into a coherent replication–segregation cycle has never been addressed and motivated this study. Our analysis has revealed that the *B. subtilis* chromosome follows an unexpected and previously unidentified choreography during vegetative growth in which the organization alternates between *ori-ter* and left-*ori*-right patterns. Our data further suggest that the highly conserved partitioning system (*parABS*) and the structural maintenance of chromosomes (SMC) condensin complex, in conjunction with replication initiation, function as the core components for this oscillating cycle. We propose that this cycle enhances the efficiency of DNA replication and sister chromosome segregation and provides a unifying model for the diverse patterns of chromosome organization observed in bacteria.

Results

Sporulating *B. subtilis* Chromosomes Have an *ori-ter* Organization. As a first step toward our analysis of chromosome organization in *B. subtilis*, we modified the cytological tools to visualize chromosomal loci in live cells. Previous fluorescently tagged repressor proteins bound to operator arrays caused partial or complete blocks to replisome progression in *B. subtilis* (15, 22, 23). We reduced the number of binding sites in the arrays and lowered expression of the repressor protein fusions using a weak constitutive promoter (*Materials and Methods*). Under these conditions, virtually all cells contained fluorescent foci with no detectable impact on growth rate, nucleoid morphology, or nucleoid size distribution (Fig. S1).

Significance

In bacteria, faithful and efficient DNA segregation is intimately linked to the spatial organization of the chromosome. Two distinct organization patterns have been described for bacterial chromosomes (*ori-ter* and left-*ori*-right) that appear to arise from distinct segregation mechanisms. Here, we show that the *Bacillus subtilis* chromosome oscillates between them during a replication–segregation cycle. Our data further suggest that the highly conserved condensin complex and the *parABS* partitioning system function as the core components that underlie these alternating patterns. We propose that this oscillatory cycle enhances the efficiency of DNA replication and sister chromosome segregation and provides a unifying model for the diverse patterns of chromosome organization observed in bacteria.

MICROBIOLOGY

PNAS

To validate these tools, we analyzed the organization of the replicated chromosomes during spore formation. At early stages in this developmental process, the replicated chromosomes adopt a structure called the axial filament, in which the origins are anchored at the cell poles and the termini are present near midcell (16, 24–26). We visualized six chromosomal loci [−7° (*ori*) and ±87°, ±120°, and +174° (*ter*)] during sporulation and determined their population-average, normalized position relative to cell length using automated image analysis software (27) (Fig. 1 *A–E*). The origins were present close to the cell poles at 0.17 and 0.83, and the termini were located at midcell (0.5). The ±87° and ±120° loci localized linearly between them. These results confirm and extend previous observations (24, 25, 28) that the sporulating chromosomes are organized linearly along their length from the poles to midcell in a *C. crescentus*-like *ori-ter ter-ori* organization (Fig. 1*B*).

***B. subtilis* Maintains a Partially Diploid State.** The analysis of chromosome organization in *C. crescentus* and slow-growing *E. coli* was facilitated by their simple cell cycles with no overlapping rounds of replication (3, 12, 13). When grown in rich media, *B. subtilis*, like *E. coli*, undergoes multifork replication and the cells are born with partially replicated chromosomes. In defined rich medium [doubling time (τ) = 35 min], the cells were born with two origins

and, on average, the number of origins per cell was 3.1 (n = 1,825) (Fig. 1*F*). To obtain a simpler DNA replication cycle, we grew *B. subtilis* in minimal medium supplemented with different carbon sources, as was done previously in *E. coli*, to reduce growth rate and DNA content. Although we could slow growth in glucose (τ = 48 min), succinate (τ = 77 min), and sorbitol (τ = 98 min), under all conditions tested, the cells were born with two origins, and the average number of origins per cell was 2.8, 2.3, and 2.1 (n > 1,700), respectively (Fig. 1*G* and Fig. S2*A*). Even under the slowest growth condition, cells were born with greater than 50% of their chromosome replicated (Fig. S2*B*). Thus, we were unable to identify conditions in which cells are born with a single unreplicated chromosome (1-N content). These results suggest that there is a link between DNA replication and cell division that ensures cells are born with two almost completely replicated chromosomes under normal growth conditions, a requirement for successful sporulation. We therefore initiated our analysis using conditions in which cells were artificially restricted to a single copy of the chromosome by inhibiting replication initiation.

Left-*ori*-Right Chromosome Organization in Cells with a Single Chromosome. To analyze vegetatively growing cells with 1-N DNA content, we inhibited replication initiation using a temperature-sensitive mutant of the helicase loader (DnaB) (29, 30). Cells were grown in rich medium at the permissive temperature (30 °C, τ = 57 min) to early exponential phase and then shifted to the restrictive temperature (42 °C, τ = 33 min) (Fig. 2*A*). After 1 h, 84% of the cells (n = 1,224) had a single-lobed nucleoid containing one replication origin, indicating that the chromosome content was reduced to 1-N (Fig. 2*A*). After 1.5 h, >90% of the cells (n = 2,399) had a single origin. Furthermore, as observed previously by McGinness and Wake (31), the nucleoids adopted a bilobed structure (Fig. 2*A*). Strikingly, in most cases (92%, n = 2,196), the origin was located at or close to the center of the two lobes (Fig. 2 *A*, *C*, *D*, and *F*). This localization pattern is dramatically different from sporulating cells, in which origins are at the extreme poles (Fig. 1*C*), and vegetatively growing cells with unperturbed replication, in which origins are frequently localized at the nucleoid periphery (14, 16) (Fig. 1 *F* and *G* and Fig. S2*A*). To determine whether each nucleoid lobe represents a chromosome arm, we visualized pairs of loci on the left and right arms. Eighty percent of the cells (n = 1,633) with fluorescently tagged loci at ±87° and 88% of the cells (n = 1,634) with tagged loci at ±120° had these markers in separate nucleoid lobes (Fig. 2 *B* and *E*). We also monitored loci at −87° and −120° on the same chromosome arm. In 86% of the cells (n = 1,804), the two loci were present in the same nucleoid lobe (Fig. 2 *B* and *E*). Furthermore, in the majority of these cells, the −87° locus was closer to the center of the two lobes and the −120° locus was closer to the nucleoid edge (Fig. 2 *B* and *E*).

Analysis of a locus close to the replication terminus (+174°) revealed that most cells had a *ter* locus directly between the two lobes (64%, n = 2,196) or in close proximity to this position (17%) (Fig. 2 *C* and *F*). However, in 18% of the cells, the terminus was present near the edge of the nucleoid. To visualize a larger region of the terminus, we used YFP fusion to the replication termination protein (RTP) (32). RTP binds to nine termination sites spanning ~430 kb of the terminus region (33). RTP-YFP localized as a single focus, clusters of foci, or multiple foci spanning the bilobed nucleoid (Fig. 2*D*), consistent with the terminus region connecting the ends of the two lobes. Similar results were obtained using different strain backgrounds and different growth media, as well as when initiation was blocked using *dnaA*(ts) or induction of SirA, an inhibitor of DnaA (34, 35). Collectively, these data indicate that under conditions in which *B. subtilis* is restricted to 1-N content, the nucleoid is organized in a pattern like the *E. coli* chromosome during slow
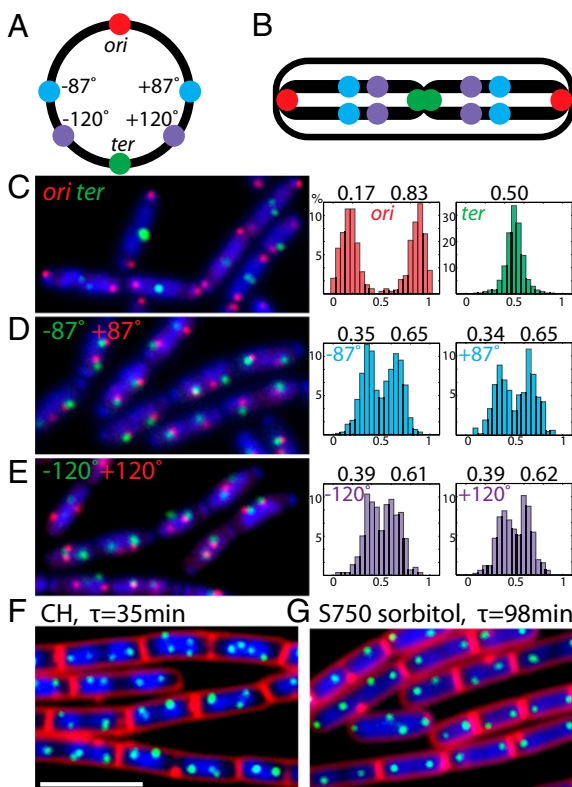

Fig. 1. Chromosome organization during sporulation. (*A–E*) Exponentially growing cells were induced to sporulate and imaged after 2 h. All strains contained a mutation in *spoIIIE* (*spoIIIE36*) (55) to prevent DNA transport. (*A*) Chromosome map showing positions of operator arrays. (*B*) Schematic summary of cellular localization of loci. Representative micrographs of cells labeled with pairs of loci *ori-ter* (*C*, *Left*), ±87° (*D*, *Left*), and ±120° (*E*, *Left*) are shown. (*C–E*, *Right*) Loci position relative to cell length analyzed (*Materials and Methods*). The centroid of the Gaussian distribution is shown on the top of each histogram. (*F* and *G*) Origin number and localization in rich and poor growth media. Origins (green, *tetO48*/TetR-CFP), nucleoid (blue, HBsu-mYpet), and membrane [red, *N*-(3-triethylammoniumpropyl)-4-(6-(4-(diethylamino) phenyl) hexatrienyl), pyridinium dibromide (FM4-64)] are shown. (Scale bar: 4 µm.)
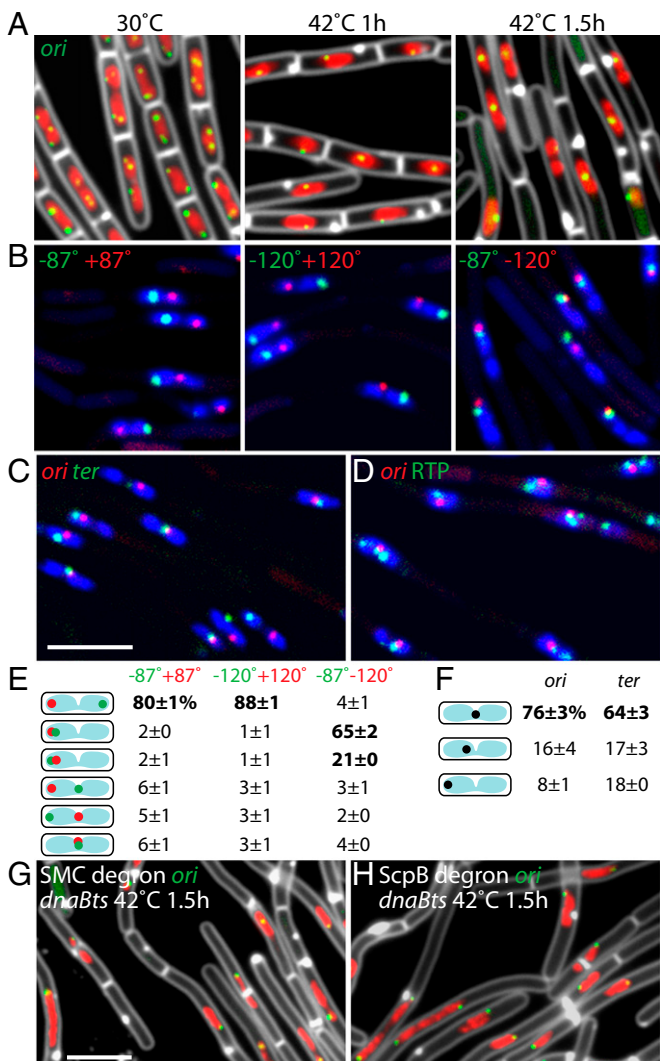
Fig. 2. Left-*ori*-right organization in cells with a single chromosome. Cells with a *dnaB*(ts) mutation were shifted from 30 °C to 42 °C for 1.5 h to block new rounds of initiation. (*A*) Origin localization before and after temperature shift. Origins (green), nucleoid (red), and membrane (white) are shown. (*B*) Representative micrographs of cells labeled at pairs of loci: ±87° (*Left*), ±120° (*Center*), and −87° and −120° (*Right*). (*C*) Cells labeled at *ori* (red) and *ter* (green). (*D*) Cells labeled at *ori* (red) and expressing RTP-YFP (green). (*E* and *F*) Quantitative analysis of loci positions. Origin localization in *dnaB*(ts) 1.5 h after temperature shift and degradation of SMC (*G*) or ScpB (*H*) is shown. (Scale bars: 4 μm.)

growth, with the two arms present on either side of the origin and genetic loci arranged linearly from the middle toward the poles. Finally, the terminus region connects the two ends.

Origin-Localized SMC Complexes Are Required for Left-*ori*-Right Organization. In *E. coli*, the left-*ori*-right organization is shifted to an *ori-ter* pattern in cells lacking the condensin complex MukBEF (36, 37). We used degradable variants of *B. subtilis* SMC or its partner protein ScpB to investigate whether the left-*ori*-right organization similarly depends on the condensin complex. Degradation of SMC (and ScpB separately) was induced when *dnaB*(ts) cells were shifted to the restrictive temperature to block replication initiation. After 1.5 h, 91% of SMC-degraded cells (*n* = 1,005) had a more extended chromosome structure, with the replication origin located at the extreme edge of the nucleoid (Fig. 2*G* and Fig. S3). Similar results were obtained after ScpB degradation (Fig. 2*H*).

The Spo0J (ParB) protein in *B. subtilis* has been shown to recruit SMC complexes to the origin region (28, 38). Accordingly, we investigated the organization of the nucleoid in its absence (Fig. S3). In the majority of the Spo0J mutant cells (70%, *n* = 999), the origin of replication localized to the edge of the nucleoid. This phenotype was principally due to the absence of Spo0J-mediated recruitment of SMC rather than the loss of the *parABS* partitioning activity, because cells lacking Soj (ParA) that are not impaired in SMC recruitment (28) retained the left-*ori*-right pattern (Fig. S3). We conclude that origin-localized condensin complexes play a critical role in generating the *E. coli*-like pattern.

***ori-ter* and Left-*ori*-Right Patterns Alternate During the Replication–Segregation Cycle.** The two distinct patterns of chromosome organization described above were observed under extreme conditions. In one, the origins were physically tethered to the cell poles during bacterial differentiation (24, 26); in the other, replication initiation was blocked and the cells were restricted to 1-N content. To investigate whether exponentially growing cells with unperturbed DNA replication possess either pattern, we used time-lapse fluorescence microscopy to visualize chromosomal loci during replication–segregation cycles. To ensure the best time resolution, we used minimal medium supplemented with sorbitol (τ = 98 min). First, we visualized the origin (Fig. 3*A*). The cells were born with two origins at opposite edges of the nucleoid and remained at the nucleoid periphery for the rest of the replication cycle. Previous studies suggested that replication initiates in the middle of the nucleoid (15, 20). However, in our movies, the origin foci became brighter at or close to the nucleoid periphery, indicative of their replication at this site (Fig. 3*A* and Fig. S4*A*, red carets). Similarly, in snapshot images, replisomes colocalized with the brighter origin foci at the nucleoid edge (Fig. S4*B*). Shortly after their replication, the two new origins migrated as a unit to the middle of the nucleoid (Fig. 3*A* and Fig. S4*A*, yellow carets). This event was followed by their bidirectional segregation to opposite edges of the nucleoid. This cycle is consistent with snapshot images in which most cells have two origins at the outer edges of the nucleoid (16, 19) (Fig. 1 *F* and *G* and Fig. S2*A*).

Next, we tracked markers on the left and right chromosome arms. For most of the cell cycle, the ±87° loci localized adjacent to each other. However, for a brief period (20–30 min), the two loci separated, localizing on either side of the nucleoid (Fig. 3*B*, black arrow, and Fig. S5). After this period of resolution, the two loci were replicated, segregated, and colocalized again. Similar results were obtained for the pair of markers at ±120°. To relate the dynamic movement of the markers on opposite arms to the replication cycle, we used mCherry–Spo0J (ParB) fusion to localize the origin (14) while simultaneously following the markers at ±87°. When the ±87° markers colocalized, the origin was almost always present at the edge of the nucleoid (Fig. 3*C*). However, when the ±87° markers were spatially resolved, the replicated origins were either in the middle of the nucleoid between the ±87° markers or had already segregated to the edges of the nucleoid (Fig. 3*C*). Thus, movement of the duplicated origins to midcell is accompanied by resolution of the left and right arms. This unprecedented choreography can explain some of the unusual localization patterns observed previously (15, 19) and is fully supported by snapshot images in which we visualized fluorescently labeled replisomes and an origin locus (Fig. S6).

Combining the time-lapse microscopy, the three-color images, and the replisome localization relative to the origin, a picture emerges of the replication–segregation cycle in *B. subtilis* (Fig. 4). At birth, the two origins are located at opposite edges of the nucleoid, with the partially replicated arms lying side by side. At the time of the next round of initiation, replisomes assemble on the polarly localized origins. The newly replicated origins then migrate as a unit to the middle of the nucleoid. At this time, the unreplicated chromosome arms become spatially resolved and
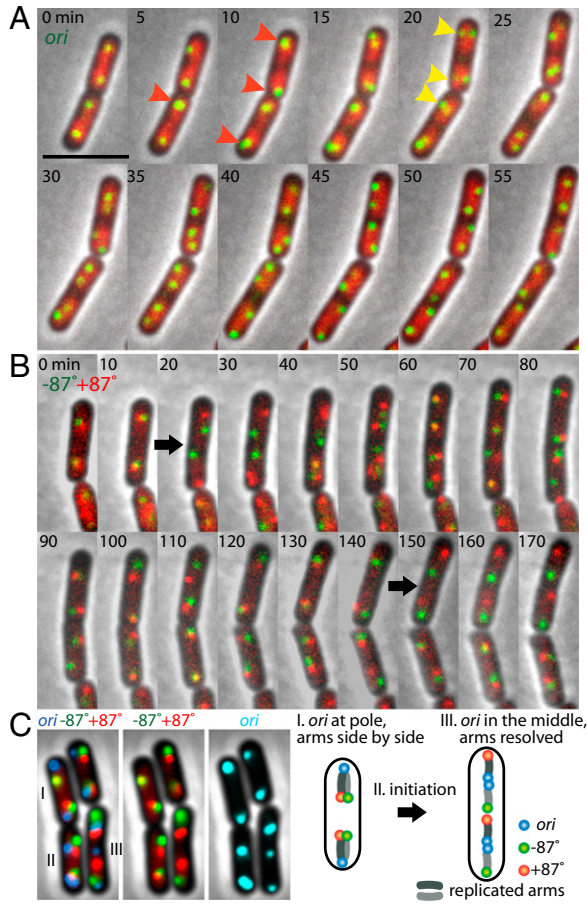
Fig. 3. Alternating patterns of chromosome organization during the cell cycle. (*A*) Time-lapse progression (5-min intervals) of cells labeled at the origin (green) and nucleoid (red) grown in minimal medium supplemented with sorbitol. Red carets highlight replication initiation at the edge of the nucleoid. Yellow carets show duplicated origins at the center of the nucleoid before their segregation. (*B*) Time-lapse progression (10-min intervals) of cells labeled at −87° (green) and +87° (red). Black arrows highlight resolution of the left and right loci. (*C*) Representative micrograph of cells labeled at three chromosomal loci: origin (blue, mCherry-Spo0J), −87° (green), and +87° (red). Stages in the replication–segregation cycle are indicated (I–III) and are interpreted in the schematic model (*Right*). Origin, −87°, and +87° loci are labeled as blue, green, and red balls, respectively. Chromosome arms are shown as gray lines. (Scale bar: 4 μm.)

the replisomes track independently of each other along them (Fig. S7). The left-*ori*-right pattern of the template DNA persists even after the origins are segregated to the nucleoid periphery and only returns to the *ori-ter*–like organization after the arms themselves have been replicated.

Partitioning Locus Helps Establish and Maintain the Origins at the Nucleoid Edge. We investigated whether the *B. subtilis* partitioning locus is responsible for maintaining the origins at the nucleoid periphery until the next round of replication. Chromosomally encoded *par* loci are composed of an ATPase (ParA), a DNA binding protein (ParB), and a centromere-like sequence (*parS*) (39). All three are critical for origin segregation in *C. crescentus* (40, 41), *Pseudomonas aeruginosa* (42), and *V. cholerae* chromosome II (43). In *B. subtilis*, cells lacking ParA, called Soj, have a very mild defect in chromosome segregation (23). ParB mutants have a more pronounced phenotype, but this is thought to be a consequence of a failure to enrich SMC complexes at the origin (23, 28, 38). Accordingly, for these experiments, we used a Soj

(ParA) mutant that has no apparent impact on origin-localized SMC (28). Analysis of origin dynamics in cells lacking Soj revealed that the directional movement of the newly replicated origins was abolished (Fig. 5 *A* and *C* and Fig. S8). Instead of segregating to the edge of the nucleoid (Figs. 3*A* and 5*B* and Fig. S8), the origins moved more slowly and in an irregular manner (Fig. 5 *A* and *C* and Fig. S8). Although they reached the nucleoid edge, they frequently moved back toward midcell.

Next, we investigated whether Soj helps maintain the two chromosomal arms adjacent to each other in an *ori-ter* pattern. Time-lapse imaging of markers at ±87° in the Δ*soj* mutant revealed that these loci remain resolved for the majority (62 ± 8%) of the replication cycle (*n* = 100) (Fig. 5*D* and Figs. S9 and S10*B*). By contrast, in WT cells, these loci were resolved for only 37 ± 7% (*n* = 100) of the replication cycle (Figs. 3*B* and 5*D* and Figs. S5 and S10*A*). Furthermore, instead of alternating between arm colocalization and arm resolution as observed in WT cells (Figs. 3*B* and 5*D* and Figs. S5 and S10*A*), the Δ*soj* mutant had more dynamic arm movements, with irregular patterns of arm colocalization and resolution (Fig. 5*D* and Figs. S9 and S10*B*). These data indicate that Soj, and presumably the partitioning locus, facilitates bidirectional origin segregation and plays a central role in both establishing and maintaining the *ori-ter* pattern.

Discussion

Our data support a model in which origin-localized condensin complexes and the partitioning system are the principal driving forces that underlie the two patterns described here, whereas replication initiation serves as the switch that triggers the oscillation between them. In this model, recruitment of SMC complexes to the origin by ParB (28, 38) sets up the left-*ori*-right pattern. SMC resolves the replicated origins (44, 45), and by analogy to the stiffening of eukaryotic centromeres by condensin (46), we hypothesize that SMC rigidifies the origin region constraining the left and right arms on either side of the origin through lengthwise condensation (47). Because SMC complexes are present at the origin throughout the cell cycle, force must be applied to the chromosome to generate the *ori-ter* pattern. We have shown that Soj (ParA) actively segregates origins to the nucleoid periphery and plays an important role in both establishing and maintaining this *ori-ter* organization. By analogy to chromosome and plasmid segregation in other bacteria (48, 49), we hypothesize that Soj acts by exerting pulling forces on Spo0J
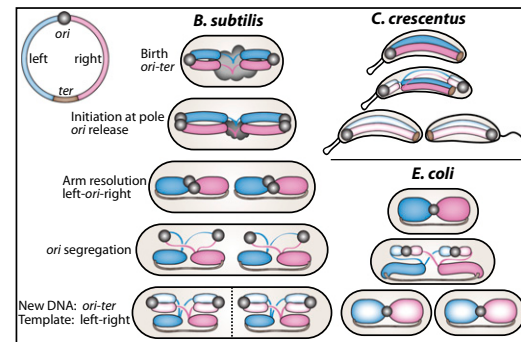
Fig. 4. Schematic model of the organization–segregation cycle in *B. subtilis*, and its comparison with *C. crescentus* and *E. coli*. Origins are represented as black balls, and termini are represented as brown lines in *B. subtilis* and *E. coli* and as a brown oval in *C. crescentus*. The compacted left and right chromosome arms are shown as thick blue and purple lines (or blobs). Newly replicated DNA is shown with a lighter hue, whereas uncompacted DNA is shown as thin lines. In the *B. subtilis*, newborn cell, unreplicated DNA is shown as a black cloud. The replication–segregation cycle of *C. crescentus* and *E. coli* corresponds to two halves of the cycle in *B. subtilis*.
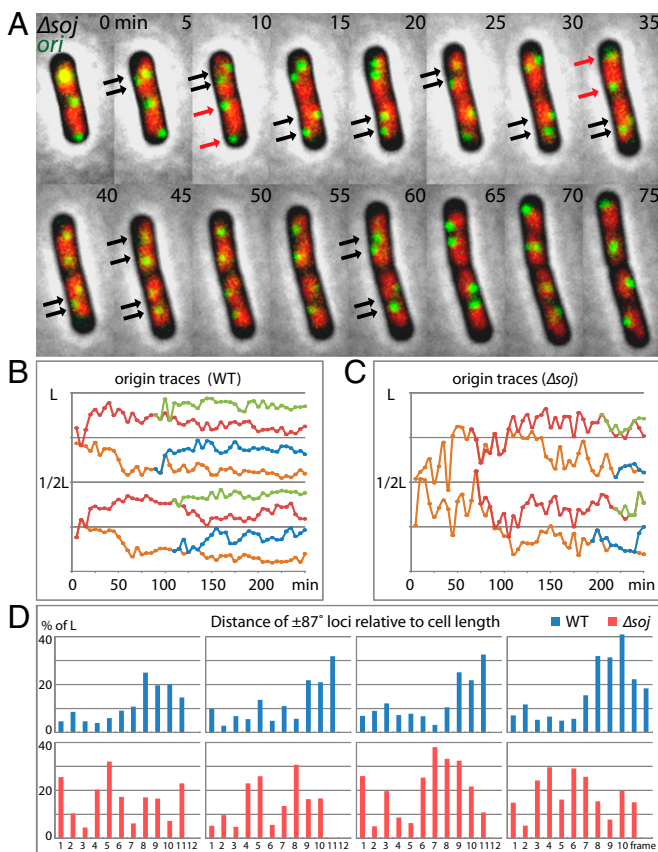
**Fig. 5.** Impaired origin segregation and chromosome arm dynamics in the absence of Soj (ParA). (*A*) Time-lapse progression (5-min intervals) of Δ*soj* cells. The origin (green) and nucleoid (red) are shown. Representative origin traces in WT (*B*) and Δ*soj* (*C*) are shown. The position of the origin was plotted relative to the total cell length (Fig. S8). (*D*) Interfocal distances of ±87° loci are analyzed in representative WT (*Upper*) and Δ*soj* (*Lower*) cells in time-lapse progressions (10-min intervals). Each graph plots the distance between a pair of ±87° loci relative to the cell length (L) at indicated times during their replication cycle. For the purpose of this analysis, the replication cycle of these loci begins when both ±87° loci are replicated (defined as frame 1) and finishes when either of the two loci is replicated again. Because each cell has two pairs of ±87° loci in its replication cycle, the maximum distance of a pair of ±87° loci is 50% of the cell length (Fig. S10).

(ParB) bound to *parS* adjacent to the origin. Finally, we propose that replication initiation triggers the change in organization pattern by transiently inactivating the forces exerted on the origins. One possibility is that Soj's role in replication initiation (50) could temporarily relax its segregation function. Alternatively or in addition, replication of the origin region could inactivate the partitioning system by transiently disrupting the Spo0J–*parS* complexes. When force on the origins is lost, the chromosome resolves into its SMC-mediated left-*ori*-right pattern. Par-mediated segregation of the newly replicated origins initiates a new round of this oscillatory cycle. Intriguingly, in cells that are blocked for replication initiation, the partitioning system appears to become inactivated, leading to a stable left-*ori*-right configuration (Fig. 2). Chronic inhibition of replication initiation could maintain Soj in its replication-active state (50), resulting in a sustained loss of its segregation function. Alternatively, the loss of partitioning activity could be due to a change in the dynamic properties of the partitioning system (8, 11, 39, 48, 49) resulting from a reduced chromosome content in an enlarged cellular compartment. Systematic analysis of chromosome organization in *P. aeruginosa* (42) suggests that its replication–segregation

cycle could follow an alternating pattern similar to the one described here. Interestingly, this bacterium contains both condensin complexes and the Par system, and it does not anchor its origins at the cell poles. Furthermore, recent quantitative analysis of snapshot images suggests an *ori-ter*–like chromosome organization in fast-growing *E. coli* (51). The localization of the replisome to midnucleoid zones in these fast-growing cells (51) raises the possibility that a transient left-*ori*-right intermediate might exist during these overlapping replication cycles. Time-lapse imaging of loci on both replication arms or simultaneous imaging of three loci will be required to establish whether or not this is the case.

In the cycle we report here, the template DNA adopts a left-*ori*-right organization, whereas the newly replicated DNA is segregated and organized in an *ori-ter* pattern. We hypothesize that this oscillating pattern enhances the efficiency of replication and segregation of the bacterial chromosome. The left-*ori*-right pattern ensures that the two replisomes track on the template DNA in opposite cell halves (Figs. S6 and S7), providing spatial resolution to the complex topologies that inevitably arise at the replication forks. The *ori-ter* pattern of the newly replicated DNA ensures that the sister chromosomes are segregated as far as possible from each other. Finally, in the specific case of *B. subtilis*, the partitioning system also ensures that the origins reside close to the poles, where they can be readily anchored if the cell enters the sporulation pathway (24, 26). Initiation of a new round of replication transiently blocks entry into sporulation (52), and our data suggest that it also releases the origins from their polar position, allowing the replication–segregation cycle to begin again.

Finally, our data raise the possibility that the disparate patterns of chromosome organization observed in bacteria arise from modifications to a common organization–segregation mechanism. In the case of *E. coli*, which lacks a partitioning locus, the condensin-mediated left-*ori*-right pattern is established shortly after origin segregation and this ground state is maintained throughout the replication–segregation cycle (Fig. 4). In the case of *C. crescentus*, *V. cholerae* chromosome I, and sporulating *B. subtilis*, distinct polar anchoring mechanisms "lock" chromosome organization in the *ori-ter* pattern, half of the full cycle (Fig. 4). Although the removal of the polar anchoring mechanism or addition of a *par* locus is unlikely to be sufficient to recover the second half of the respective cycles, we propose that these factors are the principal drivers in evolving distinct organization–segregation cycles.

Materials and Methods

General Methods. *B. subtilis* strains were derived from the prototrophic strain PY79 . Cells were grown in defined rich casein hydrolysate medium (53) or minimal medium (S750) (54) supplemented with 1% glucose, sorbitol, or succinate as specified. To monitor chromosome organization during sporulation, we used a mutant of the SpoIIIE DNA translocase (*spoIIIE36*) that engages the forespore chromosome after polar division but is blocked in DNA transport (28, 55). Sporulation was induced by resuspension at 37 °C according to the method of Sterlini–Mandelstam (53). Images were taken 2 h after the initiation of sporulation. *E. coli* SspB protein was induced with 0.5% xylose for degradation of SsrA-tagged proteins (56). Strains, plasmids, and oligonucleotides used in this study are listed in Tables S1–S3. Strain and plasmid constructions are described in SI Materials and Methods.

Fluorescence Microscopy. Fluorescence microscopy was performed with an Olympus BX61 microscope equipped with an UPLFLN 100×/1.3-N.A. phase-contrast oil objective and a CoolSnapHQ cooled CCD camera (Photometrics) or a Nikon Ti microscope equipped with Plan Apo 100×/1.4-N.A. phase-contrast oil objective and a CoolSnapHQ² camera. Membranes were stained with trimethylammonium diphenylhexatriene (Molecular Probes) at 0.01 mM or with FM4-64 [*N*-(3-triethylammoniumpropyl)-4-(6-(4-(diethylamino) phenyl) hexatrienyl), pyridinium dibromide; Molecular Probes] at 3 μg/mL. DNA was stained with DAPI (Molecular Probes) at 2 μg/mL. Images were

cropped and adjusted using MetaMorph software (Molecular Devices). Final figure preparation was performed in Adobe Illustrator (Adobe Systems).

For snapshot imaging, cells were immobilized using 2% (wt/vol) agarose pads containing growth media. For time-lapse imaging, a glass-bottomed dish (Willco dish HBSt-5040; Willco Wells) was used as a coverslip. Exponentially growing cells were concentrated at 3,300 × g for 30 s. After removal of 90% of the supernatant, 2 μL of the culture was spotted onto the glass-bottomed dish. A 2% (wt/vol) agarose pad containing growth media was then laid on top of the bacteria. These cells were imaged on a Well Plate Holder stage (TI-SH-W; Nikon) equipped with a humid, temperature-controlled incubator (TC-MIS; Bioscience Tools). The upper face of the pad was fully exposed, allowing adequate oxygen for growth. The objective was heated using a Bioptechs objective heater system. Images were acquired every 5 or 10 min as specified. Image analyses were performed using the MathWorks MATLAB-based program MicrobeTracker (27). Details of image analysis can be found in *SI Materials and Methods*.

1. Reyes-Lamothe R, Nicolas E, Sherratt DJ (2012) Chromosome replication and segregation in bacteria. *Annu Rev Genet* 46:121–143.
2. Wang X, Montero Llopis P, Rudner DZ (2013) Organization and segregation of bacterial chromosomes. *Nat Rev Genet* 14(3):191–203.
3. Viollier PH, et al. (2004) Rapid and sequential movement of individual chromosomal loci to specific subcellular locations during bacterial DNA replication. *Proc Natl Acad Sci USA* 101(25):9257–9262.
4. Fogel MA, Waldor MK (2005) Distinct segregation dynamics of the two Vibrio cholerae chromosomes. *Mol Microbiol* 55(1):125–136.
5. Fogel MA, Waldor MK (2006) A dynamic, mitotic-like mechanism for bacterial chromosome segregation. *Genes Dev* 20(23):3269–3282.
6. Bowman GR, et al. (2008) A polymeric protein anchors the chromosomal origin/ParB complex at a bacterial cell pole. *Cell* 134(6):945–955.
7. Ebersbach G, Briegel A, Jensen GJ, Jacobs-Wagner C (2008) A self-associating protein critical for chromosome attachment, division, and polar organization in caulobacter. *Cell* 134(6):956–968.
8. Schofield WB, Lim HC, Jacobs-Wagner C (2010) Cell cycle coordination and regulation of bacterial chromosome segregation dynamics by polarly localized proteins. *EMBO J* 29(18):3068–3081.
9. Shebelut CW, Guberman JM, van Teeffelen S, Yakhnina AA, Gitai Z (2010) Caulobacter chromosome segregation is an ordered multistep process. *Proc Natl Acad Sci USA* 107(32):14194–14198.
10. Yamaichi Y, et al. (2012) A multidomain hub anchors the chromosome segregation and chemotactic machinery to the bacterial pole. *Genes Dev* 26(20):2348–2360.
11. Ptacin JL, et al. (2010) A spindle-like apparatus guides bacterial chromosome segregation. *Nat Cell Biol* 12(8):791–798.
12. Nielsen HJ, Ottesen JR, Youngren B, Austin SJ, Hansen FG (2006) The Escherichia coli chromosome is organized with the left and right chromosome arms in separate cell halves. *Mol Microbiol* 62(2):331–338.
13. Wang X, Liu X, Possoz C, Sherratt DJ (2006) The two Escherichia coli chromosome arms locate to separate cell halves. *Genes Dev* 20(13):1727–1731.
14. Lin DC, Levin PA, Grossman AD (1997) Bipolar localization of a chromosome partition protein in Bacillus subtilis. *Proc Natl Acad Sci USA* 94(9):4721–4726.
15. Webb CD, et al. (1998) Use of time-lapse microscopy to visualize rapid movement of the replication origin region of the chromosome during the cell cycle in Bacillus subtilis. *Mol Microbiol* 28(5):883–892.
16. Webb CD, et al. (1997) Bipolar localization of the replication origin regions of chromosomes in vegetative and sporulating cells of B. subtilis. *Cell* 88(5):667–674.
17. Glaser P, et al. (1997) Dynamic, mitotic-like behavior of a bacterial protein required for accurate chromosome partitioning. *Genes Dev* 11(9):1160–1168.
18. Sharpe ME, Errington J (1998) A fixed distance for separation of newly replicated copies of oriC in Bacillus subtilis: Implications for co-ordination of chromosome segregation and cell division. *Mol Microbiol* 28(5):981–990.
19. Teleman AA, Graumann PL, Lin DC, Grossman AD, Losick R (1998) Chromosome arrangement within a bacterium. *Curr Biol* 8(20):1102–1109.
20. Lemon KP, Grossman AD (1998) Localization of bacterial DNA polymerase: Evidence for a factory model of replication. *Science* 282(5393):1516–1519.
21. Berkmen MB, Grossman AD (2006) Spatial and temporal organization of the Bacillus subtilis replication cycle. *Mol Microbiol* 62(1):57–71.
22. Bernard R, Marquis KA, Rudner DZ (2010) Nucleoid occlusion prevents cell division during replication fork arrest in Bacillus subtilis. *Mol Microbiol* 78(4):866–882.
23. Lee PS, Grossman AD (2006) The chromosome partitioning proteins Soj (ParA) and Spo0J (ParB) contribute to accurate chromosome partitioning, separation of replicated sister origins, and regulation of replication initiation in Bacillus subtilis. *Mol Microbiol* 60(4):853–869.
24. Wu LJ, Errington J (2003) RacA and the Soj-Spo0J system combine to effect polar chromosome segregation in sporulating Bacillus subtilis. *Mol Microbiol* 49(6):1463–1475.
25. Bogush M, Xenopoulos P, Piggot PJ (2007) Separation of chromosome termini during sporulation of Bacillus subtilis depends on SpoIIIE. *J Bacteriol* 189(9):3564–3572.
26. Ben-Yehuda S, Rudner DZ, Losick R (2003) RacA, a bacterial protein that anchors chromosomes to the cell poles. *Science* 299(5606):532–536.
27. Sliusarenko O, Heinritz J, Emonet T, Jacobs-Wagner C (2011) High-throughput, subpixel precision analysis of bacterial morphogenesis and intracellular spatio-temporal dynamics. *Mol Microbiol* 80(3):612–627.
28. Sullivan NL, Marquis KA, Rudner DZ (2009) Recruitment of SMC by ParB-parS organizes the origin region and promotes efficient chromosome segregation. *Cell* 137(4):697–707.
29. Velten M, et al. (2003) A two-protein strategy for the functional loading of a cellular replicative DNA helicase. *Mol Cell* 11(4):1009–1020.
30. Rokop ME, Auchtung JM, Grossman AD (2004) Control of DNA replication initiation by recruitment of an essential initiation protein to the membrane of Bacillus subtilis. *Mol Microbiol* 52(6):1757–1767.
31. McGinness T, Wake RG (1979) Completed Bacillus subtilis nucleoid as a doublet structure. *J Bacteriol* 140(2):730–733.
32. Lemon KP, Kurtser I, Grossman AD (2001) Effects of replication termination mutants on chromosome partitioning in Bacillus subtilis. *Proc Natl Acad Sci USA* 98(1):212–217.
33. Griffiths AA, Andersen PA, Wake RG (1998) Replication terminator protein-based replication fork-arrest systems in various Bacillus species. *J Bacteriol* 180(13):3360–3367.
34. Wagner JK, Marquis KA, Rudner DZ (2009) SirA enforces diploidy by inhibiting the replication initiator DnaA during spore formation in Bacillus subtilis. *Mol Microbiol* 73(5):963–974.
35. Rahn-Lee L, Gorbatyuk B, Skovgaard O, Losick R (2009) The conserved sporulation protein YneE inhibits DNA replication in Bacillus subtilis. *J Bacteriol* 191(11):3736–3739.
36. Badrinarayanan A, Lesterlin C, Reyes-Lamothe R, Sherratt D (2012) The Escherichia coli SMC complex, MukBEF, shapes nucleoid organization independently of DNA replication. *J Bacteriol* 194(17):4669–4676.
37. Danilova O, Reyes-Lamothe R, Pinskaya M, Sherratt D, Possoz C (2007) MukB colocalizes with the oriC region and is required for organization of the two Escherichia coli chromosome arms into separate cell halves. *Mol Microbiol* 65(6):1485–1492.
38. Gruber S, Errington J (2009) Recruitment of condensin to replication origin regions by ParB/SpoOJ promotes chromosome segregation in B. subtilis. *Cell* 137(4):685–696.
39. Gerdes K, Howard M, Szardenings F (2010) Pushing and pulling in prokaryotic DNA segregation. *Cell* 141(6):927–942.
40. Mohl DA, Gober JW (1997) Cell cycle-dependent polar localization of chromosome partitioning proteins in Caulobacter crescentus. *Cell* 88(5):675–684.
41. Toro E, Hong SH, McAdams HH, Shapiro L (2008) Caulobacter requires a dedicated mechanism to initiate chromosome segregation. *Proc Natl Acad Sci USA* 105(40):15435–15440.
42. Vallet-Gely I, Boccard F (2013) Chromosomal organization and segregation in Pseudomonas aeruginosa. *PLoS Genet* 9(5):e1003492.
43. Yamaichi Y, Fogel MA, Waldor MK (2007) par genes and the pathology of chromosome loss in Vibrio cholerae. *Proc Natl Acad Sci USA* 104(2):630–635.
44. Wang X, Tang OW, Riley EP, Rudner DZ (2014) The SMC condensin complex is required for origin segregation in Bacillus subtilis. *Curr Biol* 24(3):287–292.
45. Gruber S, et al. (2014) Interlinked sister chromosomes arise in the absence of condensin during fast replication in B. subtilis. *Curr Biol* 24(3):293–298.
46. Ribeiro SA, et al. (2009) Condensin regulates the stiffness of vertebrate centromeres. *Mol Biol Cell* 20(9):2371–2380.
47. Marko JF (2009) Linking topology of tethered polymer rings with applications to chromosome segregation and estimation of the knotting length. *Phys Rev E Stat Nonlin Soft Matter Phys* 79(5 Pt 1):051905.
48. Vecchiarelli AG, Mizuuchi K, Funnell BE (2012) Surfing biological surfaces: Exploiting the nucleoid for partition and transport in bacteria. *Mol Microbiol* 86(3):513–523.
49. Vecchiarelli AG, Hwang LC, Mizuuchi K (2013) Cell-free study of F plasmid partition provides evidence for cargo transport by a diffusion-ratchet mechanism. *Proc Natl Acad Sci USA* 110(15):E1390–E1397.
50. Murray H, Errington J (2008) Dynamic control of the DNA replication initiation protein DnaA by Soj/ParA. *Cell* 135(1):74–84.
51. Youngren B, Nielsen HJ, Jun S, Austin S (2014) The multifork Escherichia coli chromosome is a self-duplicating and self-segregating thermodynamic ring polymer. *Genes Dev* 28(1):71–84.
52. Veening JW, Murray H, Errington J (2009) A mechanism for cell cycle regulation of sporulation initiation in Bacillus subtilis. *Genes Dev* 23(16):1959–1970.
53. Harwood CR, Cutting SM (1990) *Molecular Biological Methods for Bacillus* (Wiley, New York).
54. Grossman AD, Losick R (1988) Extracellular control of spore formation in Bacillus subtilis. *Proc Natl Acad Sci USA* 85(12):4369–4373.
55. Wu LJ, Errington J (1994) Bacillus subtilis SpoIIIE protein required for DNA segregation during asymmetric cell division. *Science* 264(5158):572–575.
56. Griffith KL, Grossman AD (2008) Inducible protein degradation in Bacillus subtilis using heterologous peptide tags and adaptor proteins to target substrates to the protease ClpXP. *Mol Microbiol* 70(4):1012–1025.

Supporting Information

Wang et al. 10.1073/pnas.1407461111

SI Materials and Methods

Image Analysis. Image analyses were performed using the MathWorks MATLAB-based program MicrobeTracker (1). The outline for sporulating cells (Fig. 1 C–E) and cells in time-lapse movies (Fig. 5 B and C and Fig. S8) was determined from phase-contrast images using built-in algorithms in Microbe-Tracker. For vegetatively growing cells that grow in chains (Fig. S2), the outline of individual cells was determined using cyto-plasmic mCherry, expressed under the control of a constitutive promoter, P_{veg} (2). Nucleoid outlines (Figs. S1 and S7) were determined using the DNA fluorescent dye DAPI or fluorescent fusions to the nucleoid-associated protein HBsu (HBsu-mYpet or HBsu-mGFP). In conditions where these fluorescence signals were used for segmentation, the background fluorescence intensity was determined by averaging the fluorescence intensity in cell-free regions of the image and subtracted from the image in MetaMorph. After background subtraction, the images were inverted in MicrobeTracker and analyzed using the same method as the phase-contrast images. After segmentation, Microbe-Tracker generated a coordinate system for each cell (or nucleoid, where DAPI or HBsu fusions were used) called a mesh, in which each point was described by two coordinates: the distance to a cell pole that was randomly selected and the distance to the midline along the cell length. The mesh was used to calculate cell (or nucleoid) parameters, such as the length, width, and area.

The number and cellular position of the replisomes or chromosomal loci were detected using SpotFinder in MicrobeTracker and recorded into the cell/nucleoid mesh (Fig. 1 and Figs. S1, S2, and S7). For Fig. 1 C–E, the normalized focus position relative to the cell length was calculated and binned into 21 slices along the cell length (x axis). The height of histograms (y axis) shows the fraction of total foci that falls into each slice of the cell length. A two-peak Gaussian was fit to determine the centroid of the distribution of all foci. In Fig. 1 C–E, 570, 525, and 558 cells, respectively, were analyzed. In Fig. 1 F and G, 1,825 and 1,874 cells, respectively, from two independent experiments were analyzed.

In Fig. 2 E and F, nucleoids that contain a single unreplicated chromosome (1-N) content (a single focus for each locus) were deemed informative and were analyzed in two independent experiments for each strain. A total of 1,633, 1,634, 1,804, and 2,196 informative nucleoids were analyzed for strains labeling ±87°, ±120°, −87° and −120°, and *ori-ter*, respectively. The mean and SD between the two experiments are shown.

Plasmid Construction. pWX179 [*yycR (−7°)::tetO48 (erm)*] was generated by inserting *tetO48* [liberated with NheI and HindIII from pLAU29; a gift from I. Lau and D. J. Sherratt (Oxford University, Oxford)] into pNS043 between NheI and HindIII. pNS043 (*yycR::erm*) is an ectopic integration vector for double-crossover insertions into the *yycR* locus [a gift from N. Sullivan (Harvard Medical School, Boston) and D.Z.R.].

pWX193 [*ycgO::P_{ftsW}-tetR-cfp (spec)*] was generated by inserting *tetR-cfp* (amplified from pNS112 using oWX238 and oWX239 and digested with HindIII and BamHI) into pWX170 between HindIII and BamHI, replacing *lacI-eyfp*. pNS112 contains *amyE::P_{spoIIE}-tetR-cfp (spec)* (a gift from N. Sullivan and D.Z.R.). pWX170 contains *ycgO::P_{ftsW}-lacI-eyfp*

(*spec*). The *ftsW* promoter, P_{ftsW}, in pWX170 was amplified from genomic DNA of WT *Bacillus subtilis* using primers oWX245 and oWX246.

pWX208 [*pelB (+174°)::lacO48 (kan)*] was generated by inserting *lacO48* (liberated with EcoRI and HindIII from pLAU23; a gift from I. Lau and D. J. Sherratt) into pKM069 between EcoRI and HindIII. pKM069 (*pelB::kan*) is an ectopic integration vector for double-crossover insertions into the *pelB* locus [a gift from K. Marquis (Harvard Medical School, Boston) and D.Z.R.].

pWX340 [*dnaX_{Cter}-mypet (cat)*] was generated by inserting the C-terminal region of *dnaX* (amplified from WT genomic DNA using oWX217 and oWX329 and digested with EagI and XhoI) into pWX318 between EagI and XhoI. pWX318 contains *mypet* gene and a chloramphenicol resistance gene. The *mypet* gene originated from the plasmid RRL50 [a gift from R. Reyes-Lamothe (McGill University, Montreal)].

pWX564 [*pelB::P_{soj}-mcherry-spo0J (parS*) (tet)*] was generated by three-way ligation to insert *mcherry* (amplified from pDR201 using primers oWX774 and oWX775 and digested with HindIII and XhoI) and *spo0J(parS*)* (liberated from pKM256 using XhoI and BamHI) into pWX516 between HindIII and BamHI. pDR201 contains an *mcherry* gene that is codon-optimized for *B. subtilis*. pKM256 contains *pelB::P_{soj}-gfp-spo0J (parS*) (cat)*, where the mutated *parS** has seven synonymous changes in the 16-base *parS* site in the *spo0J* gene (3). pWX516 contains *pelB::P_{soj} (tet)*.

Strain Construction. *sacA::hbs-mypet (kan)* in BWX721 was constructed by direct transformation of a two-way ligation into *B. subtilis*, which inserts the *hbs* gene with its native promoter (amplified using primers odr198 and odr214 and digested with EcoRI and BamHI) into pWX348 between EcoRI and BamHI. pWX348 contains *sacA:: mypet (kan)*. The *mypet* gene originated from the plasmid RRL50 (a gift from R. Reyes-Lamothe).

The in-frame deletion of *parA*, called *Δsoj132* (4), which is linked to *loxP-spec-loxP* in BWX2554, was generated using methods described before (5). Specifically, BWX2538 (5) (*Δsoj132 loxP-spec-loxP* in the JH642 background) was obtained by direct transformation of an isothermal assembly product (6) into SV132 (4) to link the unmarked in-frame deletion *Δsoj132* allele to a spectinomycin resistance gene inserted between *noc* and *yyaB* (0.7 kb upstream of *Δsoj132*). The isothermal assembly reaction contained three PCR fragments: (*i*) *noc* and its upstream region (amplified from WT genomic DNA using primers oWX894 and oWX895), (*ii*) *loxP-spec-loxP* cassette (amplified from pWX466 using oWX438 and oWX439), and (*iii*) a region downstream of *noc* and upstream of *Δsoj132* containing the *yyaB* gene (amplified from WT genomic DNA using primers oWX896 and oWX897). pWX466 contains a *loxP-spec-loxP* cassette. The *Δsoj132 loxP-spec-loxP* was then backcrossed to PY79 twice. The resulting construct was sequenced across the *soj-spo0J* region using primers oWX507 and oWX508.

lacA::P_{xylA} (Ec) sspB without an antibiotic marker (*no a.b.*) in BWX1377 was obtained by transforming pWX480 (5) [*lacA::P_{xylA} (Ec) sspB loxP-erm-loxP*] to *B. subtilis* and subsequently looping out the *loxP-erm-loxP* cassette using a *cre*-expressing plasmid pDR244, which contains a spectinomycin resistance gene and a temperature-sensitive replication origin.

1. Sliusarenko O, Heinritz J, Emonet T, Jacobs-Wagner C (2011) High-throughput, subpixel precision analysis of bacterial morphogenesis and intracellular spatio-temporal dynamics. *Mol Microbiol* 80(3):612–627.

2. Fukushima T, Ishikawa S, Yamamoto H, Ogasawara N, Sekiguchi J (2003) Transcriptional, functional and cytochemical analyses of the veg gene in Bacillus subtilis. *J Biochem* 133(4): 475–483.

3. Sullivan NL, Marquis KA, Rudner DZ (2009) Recruitment of SMC by ParB-parS organizes the origin region and promotes efficient chromosome segregation. *Cell* 137(4):697–707.
4. Lee PS, Grossman AD (2006) The chromosome partitioning proteins Soj (ParA) and Spo0J (ParB) contribute to accurate chromosome partitioning, separation of replicated sister origins, and regulation of replication initiation in Bacillus subtilis. *Mol Microbiol* 60(4):853–869.

5. Wang X, Tang OW, Riley EP, Rudner DZ (2014) The SMC condensin complex is required for origin segregation in Bacillus subtilis. *Curr Biol* 24(3):287–292.
6. Gibson DG, et al. (2009) Enzymatic assembly of DNA molecules up to several hundred kilobases. *Nat Methods* 6(5):343–345.
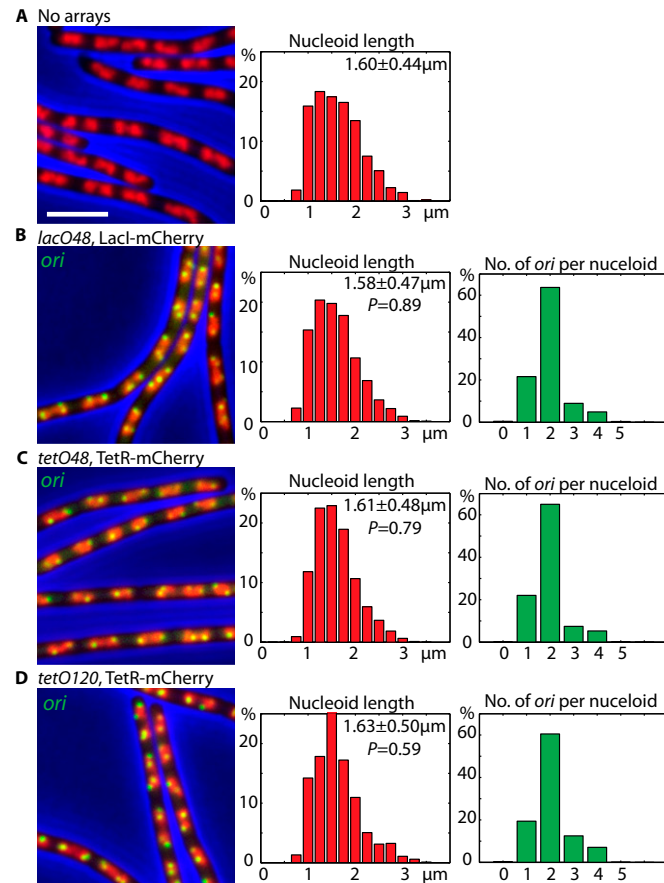
Fig. S1. *lacO* and *tetO* labeling systems do not perturb cell growth. Nucleoid length distribution and number of foci per nucleoid were compared in cells harboring no chromosome locus labeling system (*A*), *lacO48*/LacI-mCherry (*B*), *tetO48*/TetR-mCherry (*C*), and *tetO120*/TetR-mCherry (*D*). The operator arrays were inserted at the replication origin (−7°). HBsu-mGFP was used to label the nucleoid (red), and the outline and length of the nucleoid were determined using MicrobeTracker. The number of origin foci per nucleoid was determined using SpotFinder. The mean and SD of nucleoid length are displayed in the histograms. A two-sample Kolmogorov–Smirnov test was performed for nucleoid distribution in *B–D* against *A* in MATLAB, and the *P* values are displayed in the histograms. A total of 1,716, 1,478, 1,238, and 830 cells were analyzed for *A–D*, respectively. (Scale bar: 4 μm.)
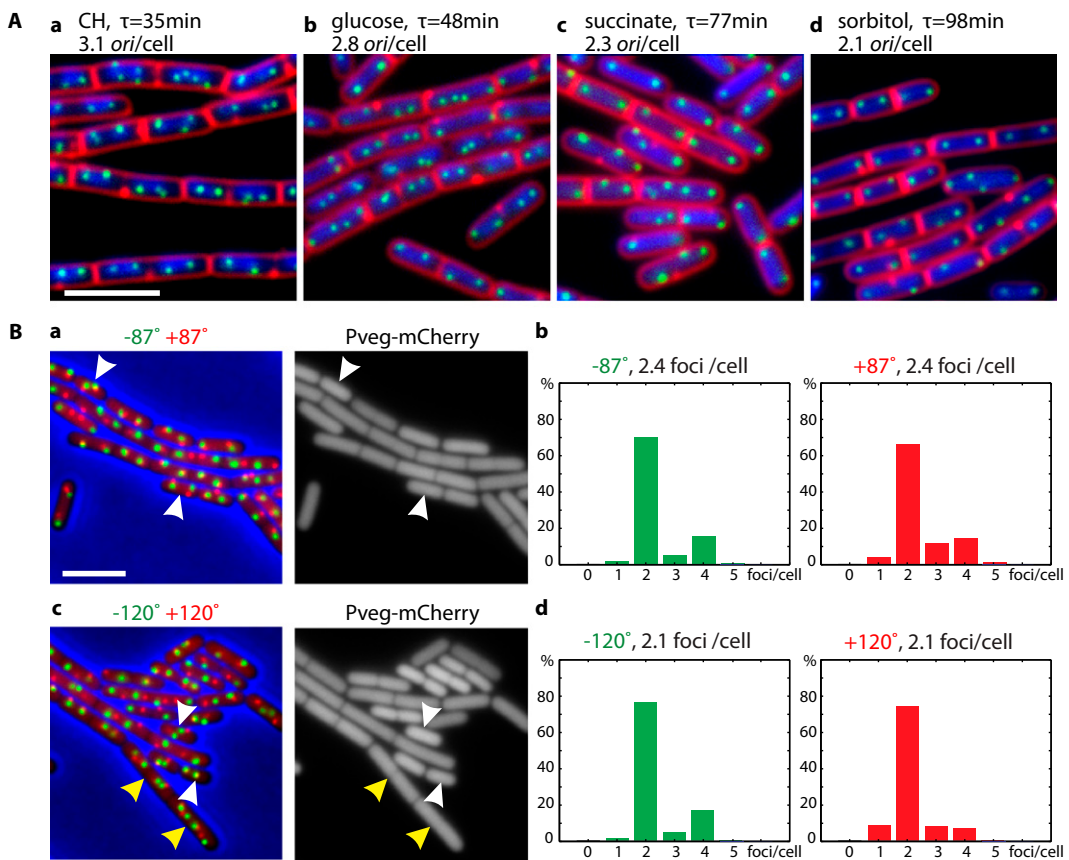
Fig. S2. *B. subtilis* maintains a partial diploid state. (*A*) Cells were born with two origins when grown in (*a*) defined rich casein hydrolysate (CH) medium or minimal medium (S750) supplemented with (*b*) glucose, (*c*) succinate, or (*d*) sorbitol. Nucleoids (blue) were labeled using HBsu-mYpet, origins (green) were labeled using *tetO48*/TetR-CFP, and membranes (red) were stained with FM4-64. τ, doubling time. The number of origins per cell was analyzed using a strain in which the origins were labeled with *tetO48*/TetR-CFP, and cytoplasmic mCherry was expressed under the control of a constitutive promoter (P_{veg}) to determine the outline of individual cells in MicrobeTracker. A description of the analysis can be found in *SI Materials and Methods*. A total of 1,825 (*a*), 1,847 (*b*), 1,736 (*c*), and 1,874 (*d*) cells were analyzed in two independent experiments. (*B*) Cells are born with greater than 50% of their chromosome replicated. Cells were grown in minimal medium (S750) supplemented with sorbitol (τ = 98 min). mCherry was expressed under P_{veg} as a cytoplasmic marker (*SI Materials and Methods*). (*B*, *a* and *b*) Chromosome loci at −87° (*lacO48*/LacI-YFP) and +87° (*tetO48*/TetR-CFP) were colored green and red, respectively. The number of foci per cell for each locus was determined using MicrobeTracker and is presented in bar graphs. The majority of cells contained two −87° loci and two +87° loci. (*B*, *c* and *d*) Chromosome loci at −120°(*lacO48*/LacI-YFP) and +120° (*tetO48*/TetR-CFP) were colored green and red. The number of foci per cell for each locus was analyzed and is presented in bar graphs. The majority of cells contained two −120° loci and two +120° loci. Examples of cells that are about to undergo cytokinesis (yellow carets) or have just completed division (white carets) are highlighted. A total of 993 (*a* and *b*) and 1,002 (*c* and *d*) cells were analyzed. (Scale bars: 4 μm.)
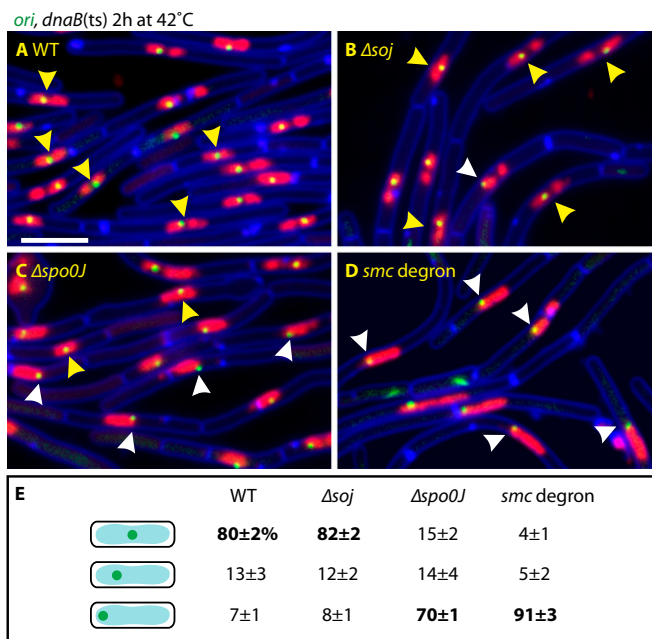
Fig. S3. Origin-localized structural maintenance of chromosome (SMC) complexes are required for left-*ori*-right organization. Origin localization was analyzed after inhibition of replication initiation in WT (*A*), Δ*soj* (*B*), Δ*spo0J* (*C*), and a strain harboring the *smc* degron (*D*). Cells were grown in rich medium (CH) at 30 °C and shifted to 42 °C for 2 h. Cultures were back-diluted to prewarmed media when necessary so that the OD_{600} was below 0.6 at all times. (*D*) Degradation of SMC-SsrA was induced with 0.5% xylose at the time of temperature shift. (*E*) Localization of the origin was quantified for nucleoids that contained a single origin. A total of 940 (*A*), 980 (*B*), 999 (*C*), and 1,005 (*D*) nucleoids from two independent experiments were analyzed, and the average and SD are shown. Yellow carets highlight the localization of the origin at or close to the center of the nucleoid. White carets show origin localization at the pole of the nucleoid. Replication origin (green) was labeled using *tetO48*/TetR-CFP. Nucleoids (red) were stained with DAPI. Membranes (blue) were stained with FM4-64. (Scale bar: 4 μm.)
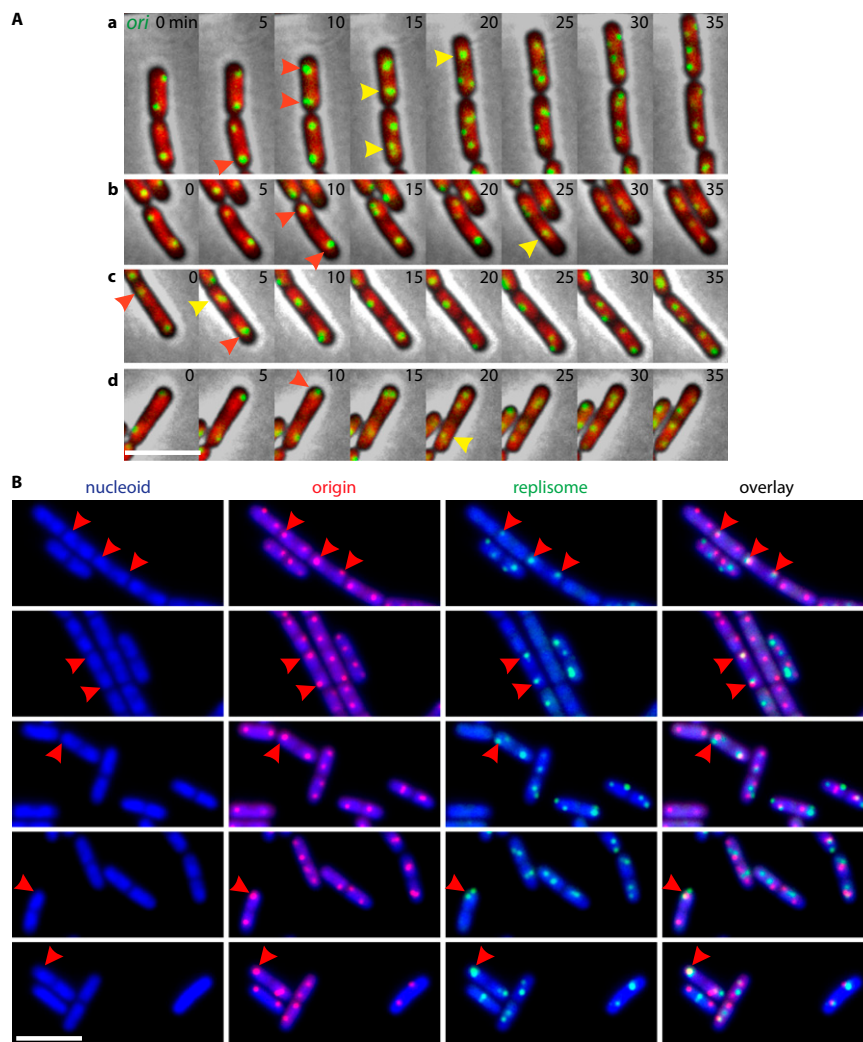
Fig. S4. Replication initiates at or near the nucleoid periphery. (*A*, *a–d*) Four representative time-lapse progressions (5-min intervals) of cells labeled at the origin (green, *tetO120*/TetR-mCherry) and the nucleoid (red, HBsu-mGFP) grown in minimal medium supplemented with sorbitol. Red carets highlight replication initiation at or close to the edge of the nucleoid, and yellow carets highlight duplicated origins at the center of the nucleoid before segregation. (*B*) Representative micrographs of cells with labeled origins (red, *tetO48*/TetR-CFP), replisomes (green, DnaX-mYpet), and nucleoids (blue, HBsu-mCherry) grown in minimal medium supplemented with sorbitol. Yellow carets highlight replication initiation at or close to the edge of the nucleoid. Cells without replisome foci have not yet initiated a new round of replication. (Scale bars: 4 μm.)
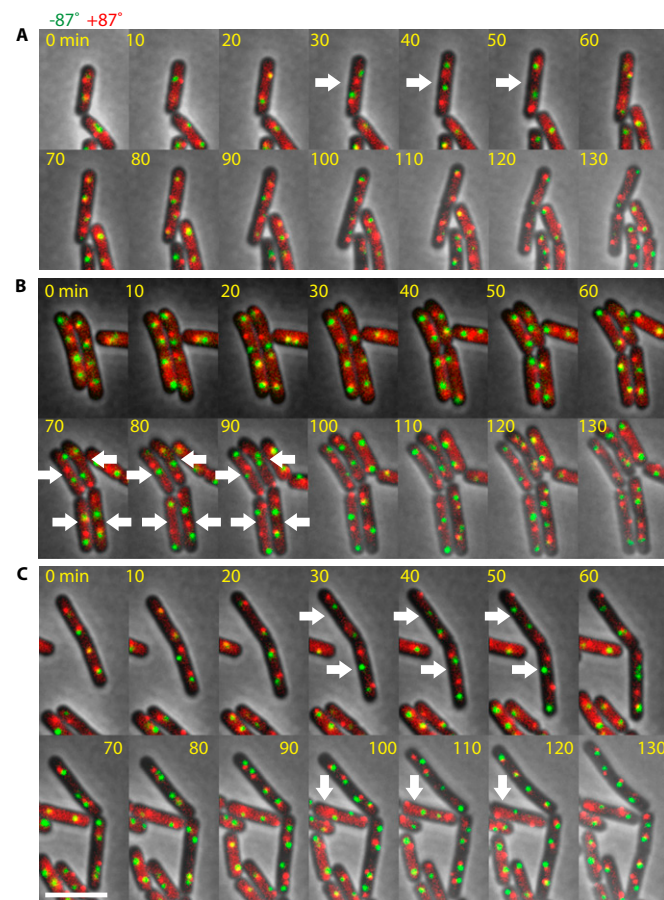
Fig. S5. Loci on separate chromosome arms resolve before their replication. (*A–C*) Three representative time-lapse progressions (10-min intervals) of cells labeled at −87° (green, *lacO48*/LacI-YFP) and +87° (red, *tetO48*/TetR-CFP). White arrows highlight the resolution of green and red foci before their replication. (Scale bar: 4 μm.)
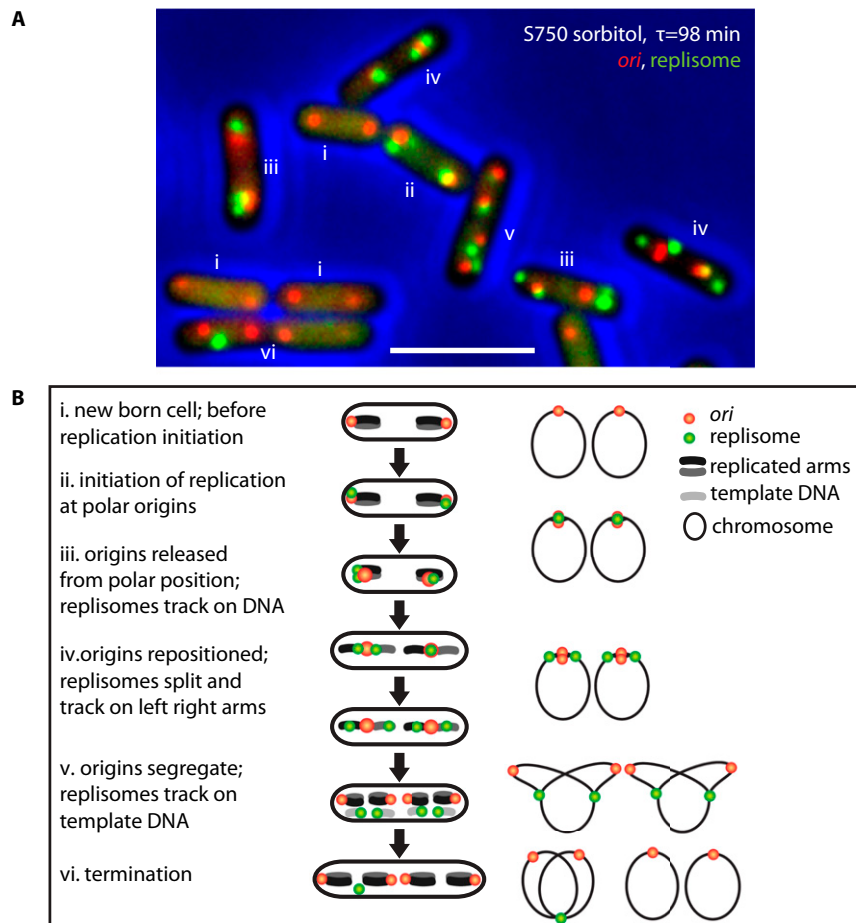
Fig. S6. Localization of the origins and replisomes in slow-growing *B. subtilis*. (*A*) Representative micrograph of origins (red, *tetO48*/TetR-CFP) and replisomes (green, DnaX-mYpet) in cells grown in minimal medium supplemented with sorbitol ($\tau = 98$ min). Numbers i–vi correspond to the deduced stages of the cell cycle as described in *B*. (Scale bar: 4 μm.) (*B*) Stages of the cell cycle. From our analysis of fields of cells from multiple snapshot images, we deduce six different stages of the cell cycle: (*i*) *B. subtilis* cells are born with a partially replicated chromosome, and the two origins localize close to the cell poles; (*ii*) replisomes form on polarly localized origins at initiation; (*iii*) replicated origins migrate as a unit from the poles to the middle of the daughter nucleoid, and replisomes track on *ori*-proximal regions, which follow the duplicated origins to the midnucleoid region; (*iv*) replisomes resolve into two foci on either side of the un-segregated origins; (*v*) origins are segregated to the edges of the nucleoid, and replisomes remain in the midnucleoid region tracking independent of each other; and (*vi*) at termination, the two replisome foci fuse and eventually disappear after replication is complete. (*Left*) Stages and the main events at each stage are described. (*Center*) Schematics of the cellular localization of the origins (red dots), replisomes (green dots), and chromosome arms (gray and beige lines) are shown. (*Right*) Structure of the circular chromosomes (black circles) at each stage is shown.
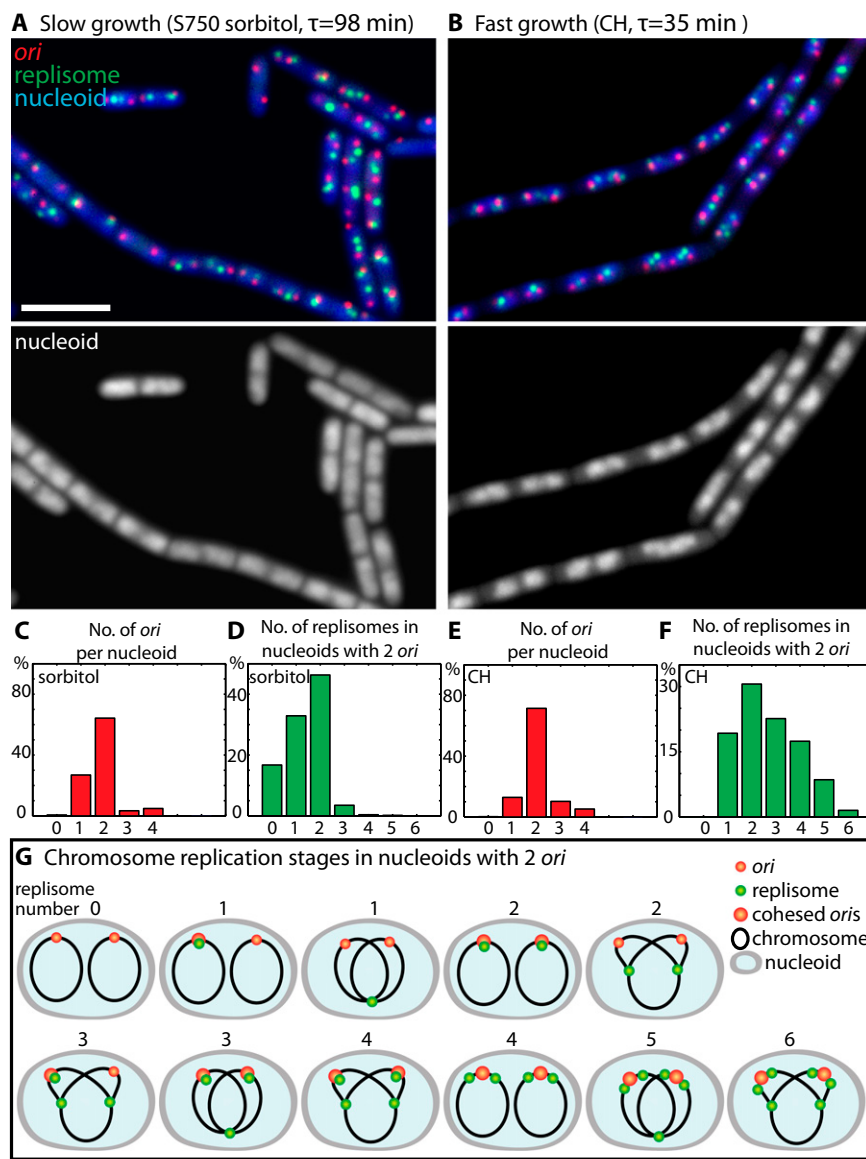
Fig. S7. Evidence that replisomes track independent of each other on separate chromosome arms. Representative micrographs of origins (red, *tetO48*/TetR-CFP), replisomes (green, DnaX-mYpet), and nucleoids (blue or white, HBsu-mCherry) in cells grown in minimal medium supplemented with sorbitol (*A*, τ = 98 min) or defined rich medium CH (*B*, τ = 35 min). (Scale bar: 4 μm.) (*C* and *E*) Nucleoids were segmented using MicrobeTracker, and the number of origin foci per nucleoid (red bars) was determined using SpotFinder. Approximately 70% of the nucleoids contained two origin foci in both conditions. (*D* and *F*) Number of replisomes in nucleoids that contained two origin foci was determined and plotted in the bar graphs (green bars). (*G*) Schematic diagrams of chromosomes at different stages of replication. The origin is shown as a small red dot, and replicated but cohesed origins are depicted as a big red dot. The replisome is illustrated as a green dot. The number of resolvable replisomes is indicated above each diagram. (*D*) Under slow-growth conditions, ~45% of the nucleoids that contain two origins have two resolved replisomes. (*F*) Under fast-growth conditions, >30% of the nucleoids that contain two origins have two resolved replisomes and ~30% have four or more replisomes. These data support a model in which replisomes track independent of each other on the two chromosome arms and are not present together in a factory. A total of 800 (*A*) and 916 (*B*) cells were analyzed.
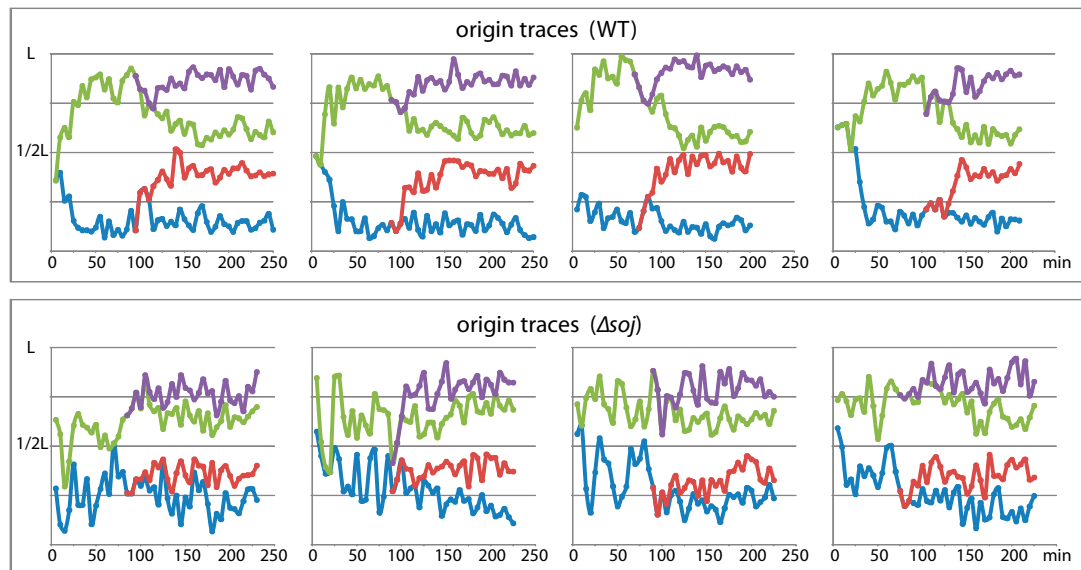
Fig. S8. Impaired origin segregation in the absence of Soj (ParA). Representative origin traces from time-lapse progressions (5-min intervals) of WT (*Upper*) and Δ*soj* (*Lower*) cells. The position of the origin was plotted relative to the total cell length (L).
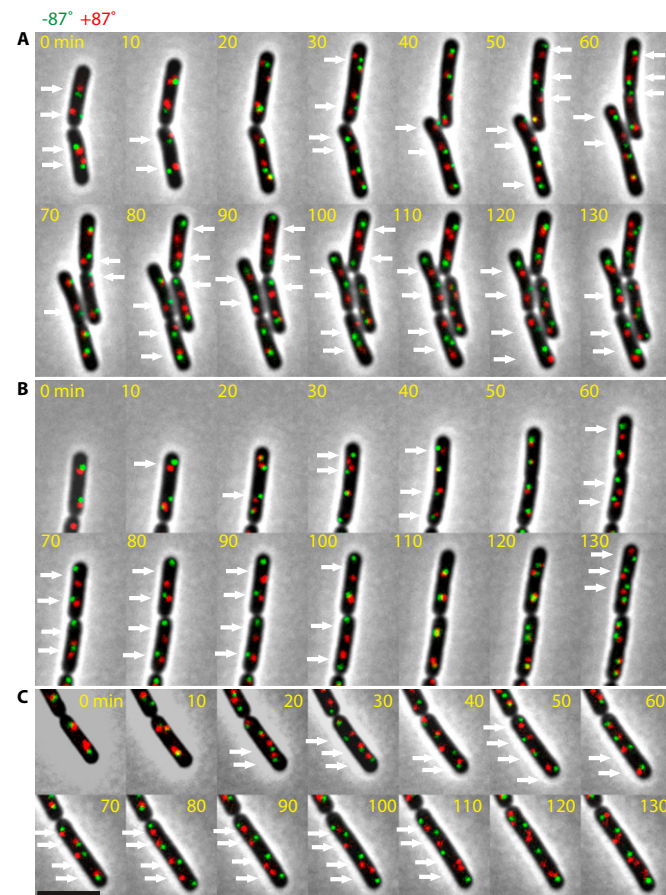
Fig. S9. Two chromosome arms remain resolved for most of the cell cycle in cells lacking Soj. (*A–C*) Three representative time-lapse progressions (10-min intervals) of cells labeled at −87° (green, *lacO*/LacI-GFP) and +87° (red, *tetO*/TetR-mCherry). White arrows highlight the resolution of green and red foci. (Scale bar: 4 μm.)

Fig. S10. Chromosome arms are disorganized in the Δ*soj* mutant. Interfocal distances of ±87° loci are analyzed in representative WT (*A*) and Δ*soj* (*B*) cells in time-lapse progressions (10-min intervals). Each graph plots the distance between a pair of ±87° loci relative to the cell length at indicated times during their replication cycle. For the purpose of this analysis, the replication cycle of these loci begins when both ±87° loci are replicated (defined as frame 1) and finishes when either of the two loci is replicated again. Because each cell has two pairs of ±87° loci in its replication cycle, the maximum distance of a pair of ±87° loci is 50% of the cell length.

Table S1. Strains used in this study

Strain	Genotype	Source	Fig.
BWX1200	*spoIIIE36, yycR(−7°)::tetO48 (cat), pelB(+174°)::lacO48 (kan), ycgO::P$_{ftsW}$ tetR-cfp (spec) terminators P$_{ftsW}$ lacI-mypet*	This study	1C
BWX1212	*spoIIIE36, yuxG(−87°)::lacO48 (phleo), yhdG(+87°)::tetO48 (cat), ycgO::P$_{ftsW}$ tetR-cfp (spec) terminators P$_{ftsW}$ lacI-mypet*	This study	1D
BWX1206	*spoIIIE36, yrvN(−120°)::lacO48 (phleo), ykoW(+120°)::tetO48 (cat), ycgO::P$_{ftsW}$ tetR-cfp (spec) terminators P$_{ftsW}$ lacI-mypet*	This study	1E
BWX721	*yycR(−7°)::tetO48 (erm), ycgO::P$_{ftsW}$ tetR-cfp (spec), sacA::hbs-mypet (kan)*	This study	1 F and G
BWX925	*yycR(−7°)::tetO48 (cat), pelB(+174°)::lacO48 (kan), ycgO::P$_{ftsW}$ tetR-cfp (spec) terminators P$_{ftsW}$ lacI-mypet, dnaB134 (ts) − zhb83::Tn917 (erm)*	This study	2 A, C, and F
BWX957	*yuxG(−87°)::lacO48 (phleo), yhdG(+87°)::tetO48 (cat), ycgO::P$_{ftsW}$ tetR-cfp (spec) terminators P$_{ftsW}$ lacI-mypet, dnaB134 (ts) − zhb83::Tn917 (erm)*	This study	2 B and E
BWX928	*yrvN(−120°)::lacO48 (phleo), ykoW(+120°)::tetO48 (cat), ycgO::P$_{ftsW}$ tetR-cfp (kan) terminators P$_{ftsW}$ lacI-mypet, dnaB134 (ts) − zhb83::Tn917 (erm)*	This study	2 B and E
BWX955	*yuxG(−87°)::lacO48 (phleo), yrvN(−120°)::tetO48 (cat), ycgO::P$_{ftsW}$ tetR-cfp (spec) terminators P$_{ftsW}$ lacI-mypet, dnaB134 (ts) − zhb83::Tn917 (erm)*	This study	2 B and E
BWX959	*yycR(−7°)::tetO48 (cat), ycgO::P$_{ftsW}$ tetR-cfp (phleo), rtp-yfp (spec), dnaB134 (ts) − zhb83::Tn917 (erm)*	This study	2D
BWX1527	*yycR(−7°)::tetO48 (cat), ycgO::P$_{ftsW}$ tetR-cfp (phleo), lacA::P$_{xylA}$ (Ec) sspB (no a.b.), smc-ssrA loxP-kan-loxP, dnaB134 (ts) − zhb83::Tn917 (erm)*	(1)	2G
BWX1377	*yycR(−7°)::tetO48 (cat), ycgO::P$_{ftsW}$ tetR-cfp (phleo), lacA::P$_{xylA}$ (Ec) sspB (no a.b.), scpB-ssrA (kan), dnaB134 (ts) − zhb83::Tn917 (erm)*	This study	2H
BWX2006	*yycR(−7°)::tetO120 (erm), ycgO::P$_{ftsW}$ tetR-mcherry (phleo), sacA::hbs-mgfp mut3 (cat)*	(1)	3A and 5B
BWX1053	*yuxG(−87°)::lacO48 (phleo), yhdG(+87°)::tetO48 (cat), ycgO::P$_{ftsW}$ tetR-cfp (kan) terminators P$_{ftsW}$ lacI-mypet*	This study	3B and 5D
BWX1930	*yuxG(−87°)::lacO48 (phleo), yhdG(+87°)::tetO48 (cat), ycgO::P$_{ftsW}$ tetR-cfp (kan) terminators P$_{ftsW}$lacI-mypet, pelB::P$_{soj}$ mcherry-spo0J (parS*) (tet)*	This study	3C
BWX2554	*yycR(−7°)::tetO120 (erm), ycgO::P$_{ftsW}$ tetR-mcherry (phleo), sacA::hbs-mgfp mut3 (cat), Δsoj132 (spec)*	This study	5 A and C
BWX2552	*yuxG(−87°)::lacO48 (phleo), yhdG(+87°)::tetO48 (cat), ycgO::P$_{ftsW}$ tetR-cfp (erm) terminators P$_{ftsW}$ lacI-mypet, Δsoj132 (spec)*	This study	5D
PY79	WT	(2)	
spoIIIE36	*spoIIIE36*	(3)	
SV132	*trpC2, pheA1, Δsoj132 (no a.b.)*	(4)	
KPL69	*trpC2, pheA1, dnaB134 (ts) − zhb83::Tn917 (erm)*	(5)	

1. Wang X, Tang OW, Riley EP, Rudner DZ (2014) The SMC condensin complex is required for origin segregation in Bacillus subtilis. *Curr Biol* 24(3):287–292.
2. Youngman PJ, Perkins JB, Losick R (1983) Genetic transposition and insertional mutagenesis in Bacillus subtilis with Streptococcus faecalis transposon Tn917. *Proc Natl Acad Sci USA* 80(8):2305–2309.
3. Wu LJ, Errington J (1994) Bacillus subtilis SpoIIIE protein required for DNA segregation during asymmetric cell division. *Science* 264(5158):572–575.
4. Lee PS, Grossman AD (2006) The chromosome partitioning proteins Soj (ParA) and Spo0J (ParB) contribute to accurate chromosome partitioning, separation of replicated sister origins, and regulation of replication initiation in Bacillus subtilis. *Mol Microbiol* 60(4):853–869.
5. Rokop ME, Auchtung JM, Grossman AD (2004) Control of DNA replication initiation by recruitment of an essential initiation protein to the membrane of Bacillus subtilis. *Mol Microbiol* 52(6):1757–1767.

Table S2. Plasmids used in this study

Plasmid	Description	Refs.
pGK97	*rtp-yfp (spec)*	(1)
pWX116S	*ykoW(+120°)::tetO48 (cat)*	(2)
pWX151	*yrvN(−120°)::lacO48 (phleo)*	(2)
pWX154	*yhdG(+87°)::tetO48 (cat)*	(2)
pWX159	*yuxG(−87°)::lacO48 (phleo)*	(2)
pWX178	*yycR(−7°)::tetO48 (cat)*	(2)
pWX179	*yycR(−7°)::tetO48 (erm)*	This study
pWX193	*ycgO::P$_{ftsW}$ tetR-cfp (spec)*	This study
pWX208	*pelB(+174°)::lacO48 (kan)*	This study
pWX340	*dnaX$_{Cter}$-mypet (cat)*	This study
pWX361	*ycgO::P$_{ftsW}$ tetR-cfp (spec) terminators P$_{ftsW}$ lacI-mypet*	(2)
pWX419	*ycgO::P$_{ftsW}$ tetR-cfp (phleo)*	(2)
pWX425	*ycgO::P$_{ftsW}$ tetR-cfp (kan) terminators P$_{ftsW}$ lacI-mypet*	(2)
pWX477	*scpB$_{Cter}$-ssrA (kan)*	(2)
pWX480	*lacA::P$_{xylA}$ (Ec) sspB loxP-erm-loxP*	(2)
pWX510	*ycgO::P$_{ftsW}$ tetR-mcherry (phleo)*	(2)
pWX564	*pelB::P$_{soj}$ mcherry-spo0J (parS*) (tet)*	This study
pWX570	*yycR(−7°)::tetO120 (erm)*	(2)

1. Lemon KP, Kurtser I, Grossman AD (2001) Effects of replication termination mutants on chromosome partitioning in Bacillus subtilis. *Proc Natl Acad Sci USA* 98(1):212–217.
2. Wang X, Tang OW, Riley EP, Rudner DZ (2014) The SMC condensin complex is required for origin segregation in Bacillus subtilis. *Curr Biol* 24(3):287–292.

Table S3. Oligonucleotides used in this study

Oligos	Sequence	Use
odr198	gccCTCGAGttttccggcaactgcgtctttaagcgc	BWX721
odr214	gccGAATTCaaatcaccttaaatccttgacgagc	BWX721
oWX217	aaaCGGCCGgtagagcggctcaaaacaacgg	pWX340
oWX238	gcgAAGCTTacataaggaggaactactatgtctagattagataaaagtaaag	pWX193
oWX239	gcgGGATCCttacttataaagttcgtccatgcc	pWX193
oWX245	gcgGAATTCtaaatgataaaactcaaacttattaacag	pWX193
oWX246	gcgAAGCTTctgcttctaacttccattatctatg	pWX193
oWX329	cgcCTCGAGtcttttatttcaattaaatccgc	pWX340
oWX438	gaccagggagcactggtcaac	BWX2554
oWX439	tccttctgctccctcgctcag	BWX2554
oWX507	cgtgcttgaattttcaattatttccc	BWX2554
oWX508	acccgttgcaaaggctcactgggcgc	BWX2554
oWX774	cgcAAGCTTacataaggaggaactactatggtc	pWX564
oWX775	tttCTCGAGtccggaacctttgtataattcgtccattccacc	pWX564
oWX894	cgcggcacagacttgatgaaacgtcc	BWX2554
oWX895	ctgagcgagggagcagaaggatccttaaaaatataaaaagctctcctgcttttc	BWX2554
oWX896	gttgaccagtgctccctggtccaaaaggtaatcacttacttttagtgaatat	BWX2554
oWX897	gatttttcccacgatgtcacctactttc	BWX2554

Restriction endonuclease sites are capitalized.